

Anisotropic wetting properties of oblique nanowires array and their applications on water transportation and fog collection

Li Cheng^a, Qi Xu^b, Xiaofeng Jia^a, Ruichao Zhang^a, Suo Bai^a, Yong Qin^{a,*}, Xudong Wang^{c,*}

^a Institute of Nanoscience and Nanotechnology, School of Physical Science and Technology, Lanzhou University, Gansu 730000, China

^b School of Advanced Materials and Nanotechnology, Xidian University, Shaanxi 710071, China

^c Department of Materials Science and Engineering, University of Wisconsin at Madison, Madison, Wisconsin 53706, USA

ARTICLE INFO

Keywords:

Anisotropic wetting
Unidirectional spread
Oblique nanowires
Water transportation
Fog collection

ABSTRACT

As a widely existing phenomenon of the surface of natural organisms, anisotropic wetting arouses much attention for their wide applications in fields as liquid transportation, fog collection, microfluidic devices and oil-water separation. Here, we presented unidirectional water spreading on the surface of oblique polyimide (PI) nanowires (NWs) array and directional moving of water droplet on hydrophobically treated oblique PI NWs array. Directional water transportation and fog collection were realized using the oblique PI NWs array. As the NWs array could be easily fabricated on PI films with our method, it is beneficial for the applications.

Introduction

Wetting phenomena such as superhydrophobic phenomenon [1–4], superhydrophilic phenomenon [4,5] and anisotropic wetting phenomenon [6–8] of some organism's surfaces and engineered surfaces are very interesting and have attracted many research interests in recent years because of its tremendous application value. Among these, anisotropic wetting properties arouse much attention for their wide applications in fields of liquid transportation [9,10], fog collection [11, 12], microfluidic devices [13] and oil-water separation [14].

In nature, anisotropic wetting phenomena were found on the surface of many organisms. Nepenthes forms a slippery liquid film on their peristome, by continuously transporting water *via* the structure on the surface of the peristome [13]. Butterflies eliminate the water droplets on their wings, with the structure on the surface of their wings, where water droplets could only roll out [15,16]. Cacti collect fog in the wind with their spines which possess complicated structure and can transport the collected water droplets to their stem [12]. Through studying these anisotropic wetting structure in natural organisms, researchers designed surfaces with anisotropic wetting properties, and achieved the applications of liquid transportation [13,17], fog collection [18,19] and so on. For example, based on principles derived from desert beetles, cacti and pitcher plants, scientists designed a structure to obtain high vapor diffusion flux and fast droplet directional transport [19]. Asymmetric structures enable water droplets spread along one or several specified

directions [6,7,20,21,22]. Besides using engineered 3D structures, scientists realized transportation of liquids along specific curves [23,24]. By applying these properties, many functional structures/devices such as liquid transportation structures [13,23,25,26], fog collection structures [18,19] and microfluidic devices [27,28] were fabricated. Despite of the remarkable progress, the on-going results are still far from practical applications, and one of the limitations is the complex process fabrication of the structures [13].

In this work, we show anisotropic wetting properties of the oblique polyimide (PI) nanowires (NWs) array, which could be easily fabricated on the entire surface of a PI film. Water droplets on the surface of the oblique PI NWs array spread against the NWs' oblique direction, even when the film was set perpendicular to ground. When the oblique PI NWs array was treated hydrophobic, water droplets could move fast against the NWs' oblique direction under vibration. Using the anisotropic wetting properties of the oblique PI NWs array, we realized water transportation on untreated oblique PI NWs array and fog collection on hydrophobically treated oblique PI NWs array. Though the oblique PI NWs array could not realize complex functions, it might be very useful in these large-scale applications which need simple manufacturing process and high production.

* Corresponding authors.

E-mail addresses: qinyong@lzu.edu.cn (Y. Qin), xudong@engr.wisc.edu (X. Wang).

<https://doi.org/10.1016/j.surfin.2020.100784>

Received 7 August 2020; Received in revised form 19 October 2020; Accepted 27 October 2020

Available online 13 December 2020

2468-0230/© 2020 Elsevier B.V. All rights reserved.

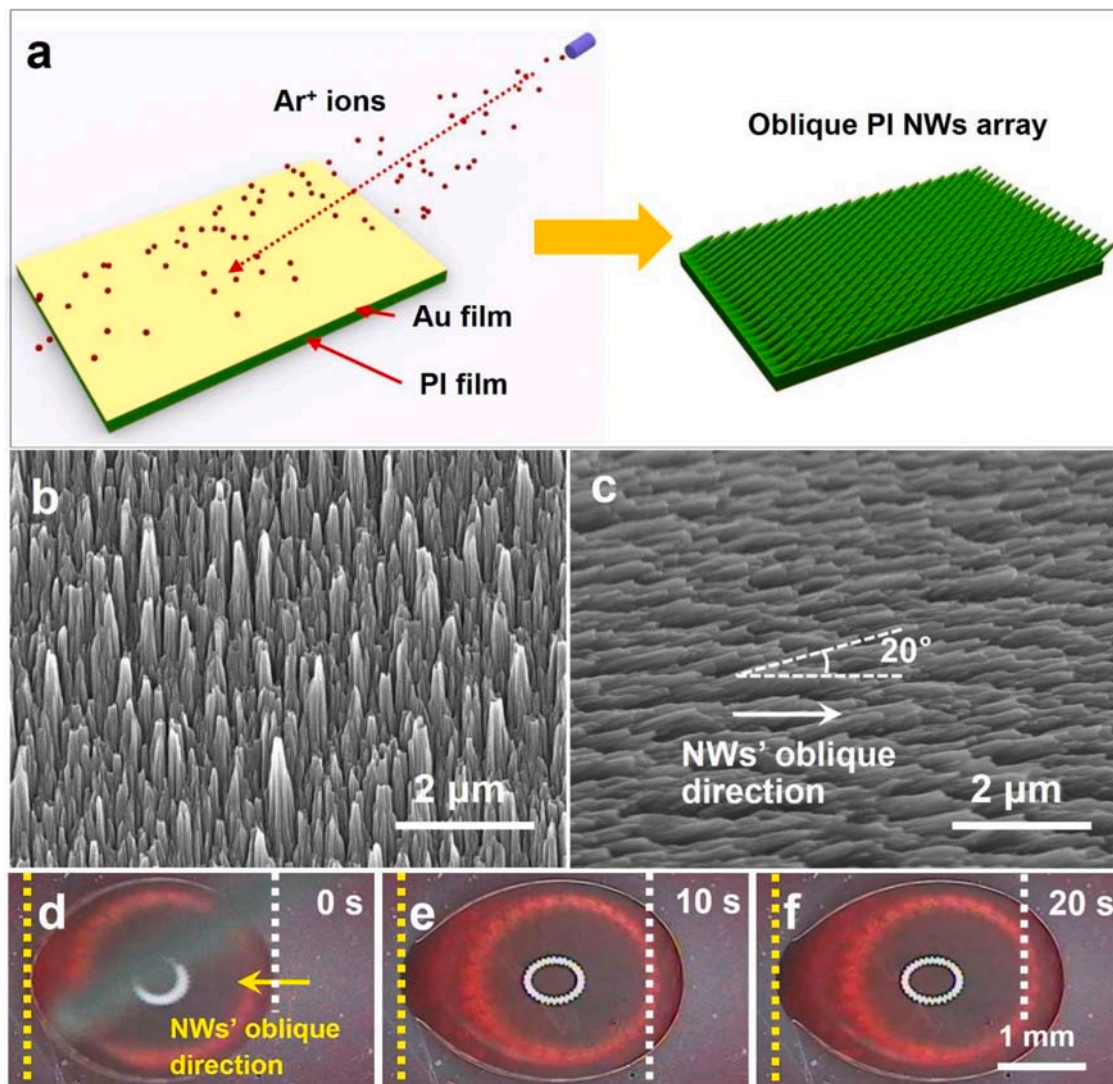


Fig. 1. Fabrication and unidirectional water spreading on oblique PI NWs array. (a) Schematic diagram of the fabrication process of oblique PI NWs array. (b) and (c) show the top view and section view SEM images of the oblique PI NWs array. (d) to (f) show the optical images of water droplet placed on oblique PI NWs array after 0 s, 10 s and 20 s, respectively.

2. Methods

Fabrication of the oblique PI NWs array [29]:

A thin film of Au (average thickness 0.4 nm) was first sputtered on a cleaning PI film, and then the film was bombarded by Ar^+ ion beam with the acceleration voltage of 4 kV. The beam current was set to 0.2 mA and the incident angle was set to 20° . After 2 hours of the bombarding process, the 20° oblique PI NWs array was fabricated on the film.

Measurement of water droplets spread on oblique PI NWs array

The PI film with oblique PI NWs array was put on a horizontal plate. Then 5 μL deionized water or SDS aqueous solution (1 g/L) was dropped on the film. The spreading process of the droplet was recorded by an optical microscope with CCD camera.

To test water spreading ability under a specific tilt angle, the film was stick onto a tilted glass slide. The tilt angle of the film was confirmed by the angle between the slide and a plumb line, and the expanding of the droplet was recorded with the same process as the horizontal condition.

Measurement of water transport on the oblique PI NWs array

The film with oblique PI NWs array was bound and fixed on a glass slide, and water was added on the film via an injection pump with a pumping speed of 1 $\mu\text{L/s}$. Moving of water on the film was recorded by an optical microscope with CCD camera.

Hydrophobic treatment of oblique PI NWs array

The diluted PDMS (1 wt% in n-octane) was spin-coated on the oblique PI NWs array at 3000 rpm for 30 s, and then heated for an hour at 80°C . Hence, the oblique PI NWs array coated with a thin film of PDMS, is hydrophobic.

Measurement of water droplet moving on hydrophobically treated oblique PI NWs array

Two pieces of the above-mentioned treated films were pasted on a horizontal plate with the NWs' oblique directions inversed to each other (in order to eliminate the possible influence of gravity). Two water droplets were respectively dropped on the surface of each film, then the films were vibrated by a loudspeaker with a voice of 400 Hz and 87 dB.

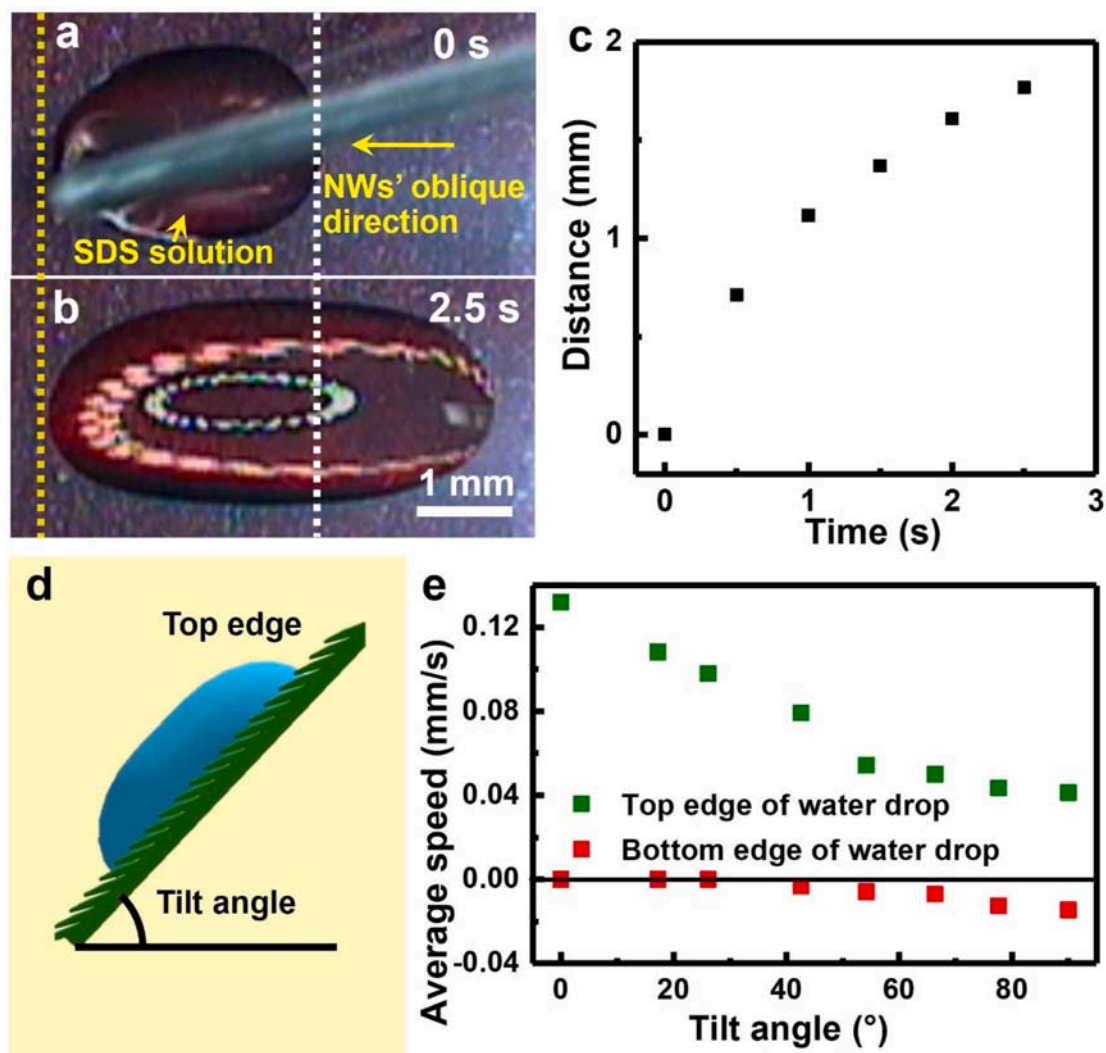


Fig. 2. Unidirectional spreading of 1 g/L SDS aqueous solution on oblique PI NWs array and of water on tilt placed oblique PI NWs array. (a) and (b) show optical images of the droplet placed on oblique PI NWs array after 0 s and 2.5 s. (c) shows the statistic result of spreading distance changing with time. (d) Schematic diagram of water placed on tilt placed oblique PI NWs array. (e) Average spreading speeds of the top edge (green squares) and bottom edge (red squares) of water in 20 s.

Moving of water droplets on the film was recorded by an optical microscope with CCD camera.

Fog collection on the hydrophobically treated oblique PI NWs array

Two pieces of the above-mentioned treated films were pasted on a horizontal plate, and the NWs' oblique direction was inverse to each other. The films were vibrated by a loudspeaker with a voice of 400 Hz and 87 dB, and fog was generated with an air humidifier and transported to the film through a rubber tube. The surface state of the film was recorded by an optical microscope with CCD camera.

Results and discussion

Fabrication of the oblique PI NWs array

As shown in Fig. 1a, the oblique PI NWs array was fabricated via an ion milling method reported in our previous work (details of the fabrication process are depicted in the methods) [29]. As shown in Fig. 1b and 1c, the obtained NWs are quite uniform possessing 20° oblique angle with the surface of the film, whose averaged length and diameter are about 1 μm and 200 nm, respectively. Moreover, in the whole area of the

film, the NWs show a nearly uniform morphology and wire density.

Anisotropic Spreading of water on oblique PI NWs array

This asymmetric structure has been proved to possess anisotropic property on many aspects [29,30], and we focused on its anisotropic wetting property in this work. As shown in Fig. 1d to 1f and Movie S1, when a water droplet is dropped on the film, the water droplet's edge spreads slowly against the NWs' oblique direction (the NWs' oblique direction is indicated by the arrow in Fig. 1c) but keeps still along other directions. In contrast, on a PI film with vertical NWs array, water droplet spreads slightly outside along all directions after dropped on the film (shown in Fig. S1). Fig. S2 shows the contact angles of water on the film, as we can see, contact angles at the side against NWs' oblique direction (79.4°) is higher than the other side (66.6°), which may be related to the reason of water spreading anisotropically on the film and the contact angles decreasing with the spreading of water droplets. This phenomenon proves that the oblique PI NWs array have the ability to control the moving behavior of the water droplets. Surface tension coefficient is one of the important parameters of liquids, which is related to behaviors of liquids. Thus, we tried to reduce the surface tension of water through adding surfactant to it. As a result, when we replace water

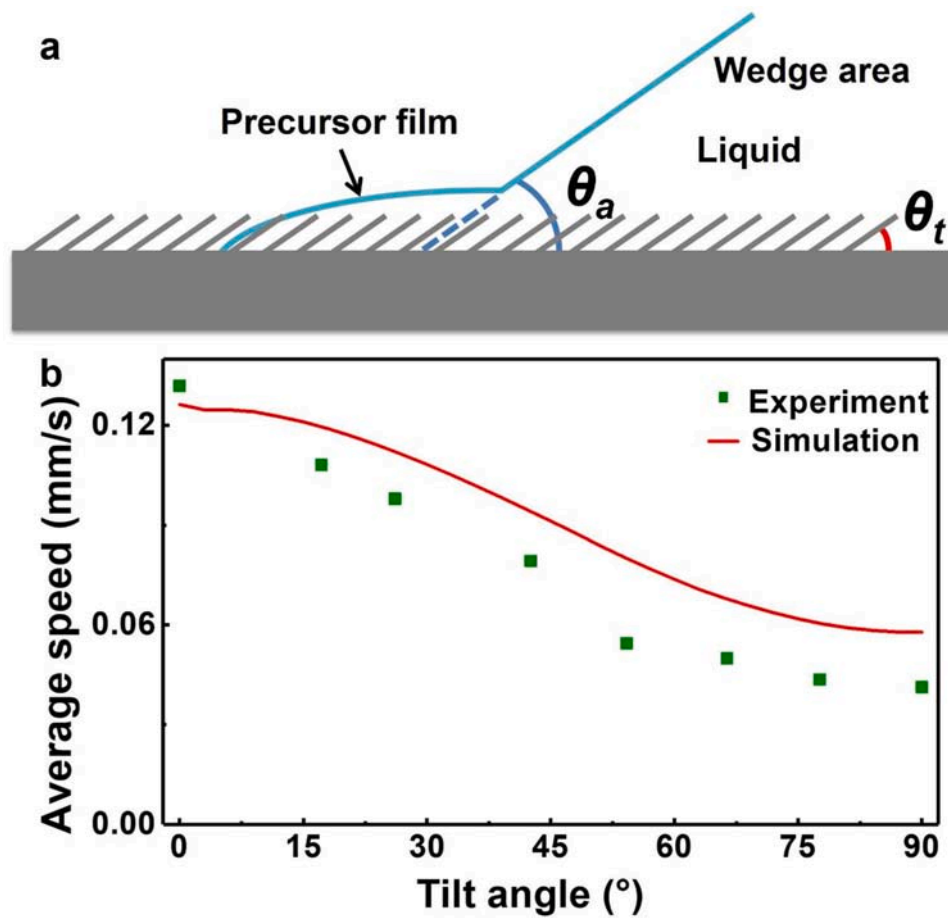


Fig. 3. (a) Schematic diagram to explain the directional spreading of water on the oblique PI NWs array, (b) simulation result of the average spreading of water against NWs' oblique direction in case of this direction tilted upward, and the corresponding experimental result.

with 1 g/L sodium dodecyl sulfate (SDS) aqueous solution in the experiment, the droplet spreads faster along that direction due to the reduced surface tension, but it is still immovable along other directions. Movie S2 shows a video of an SDS solution droplet dropping on oblique PI NWs array, and Fig. 2a and 2b show the optical images of the droplet after being placed on the oblique PI NWs array for 0 s and 2.5 s. From the video and the images we can see that the right edge of the droplet spreads gradually against the NWs' oblique direction after dropping it on the film, and the other edges of the droplet shows no observable movement. In a period of 2.5 s, the distance between the left and right side of the water droplet changes from 2.9 mm to 4.7 mm at an average speed of 0.72 mm/s. And the statistical result in Fig. 2c shows that spreading speed of the droplet decrease with time, which might be caused by the decrease of the pressure due to gravity and the increase of the horizontal component of surface tension.

The anisotropic spreading property of water on the film is further investigated by tilting the film to different angles with the horizontal plane (shown in the schematic image of Fig. 2d). Fig. 2e shows the average moving speed of top edge and bottom edge of the droplet in the first 20 s, the NWs' oblique direction was set downward in this experiment. The results show that the average speed of droplet's top edge decreases correspondingly with the increasing of tilt angle. However, the droplet could still move upward along the film even when the film was set perpendicular to the ground. On the other hand, when the tilt angle of the film is smaller than 26°, the bottom edge of the droplet keeps still. Once it is larger than 42°, the bottom edge starts expanding downward with a much slower speed than the top edge moving upward. This phenomenon indicates the effect of gravity in the spreading of water droplet, and in the meantime, there exists an asymmetric force

acting on the droplet along the droplet's spreading direction. Thus, along the droplets' spreading direction, this force enhanced the movement of the droplet; while along the NWs' oblique direction, this force hindered the movement of droplet. This asymmetric force might come from the capillary force generated by the oblique PI NWs array.

To further explain the above phenomenon, we give an interpretation based on the relationship between unbalanced Young's force which is a capillary force and three terms of dissipations (wedge dissipation, precursor film dissipation and an unknown dissipation) proposed by P. G. de Gennes. [31],

$$FU = T(\Sigma_w + \Sigma_f + \Sigma_l)$$

Here, F is the unbalanced Young's force, U is the velocity of the contact line and $T\Sigma_w$ represents the wedge dissipation which is one kind of viscous friction caused by the rolling motion of the liquid in this region. This wedge locates at a position which is about 100 μm from the nominal contact line. Ahead of this wedge exists a precursor film extending over a finite distance (Fig. 3a). $T\Sigma_f$ represents the viscous dissipation in this region. The analytical form with parameters of the above two terms has been obtained. $T\Sigma_l$ represents an unknown dissipation term which may come from the local structure.

To describe the effect of the film on the droplet's behavior, we add two other force terms to the right side of the equation. One term is the capillary force exerted by the oblique PI NWs array, which is concluded from the experimental phenomena. And another term is the gravity which is introduced to describe the droplet's behavior on a tilted substrate. As for the unknown dissipation term $T\Sigma_l$, we represent it with the oblique PI NWs array's hysteresis effect. More detailed derivation process about each term can be found in the Supplementary Information.

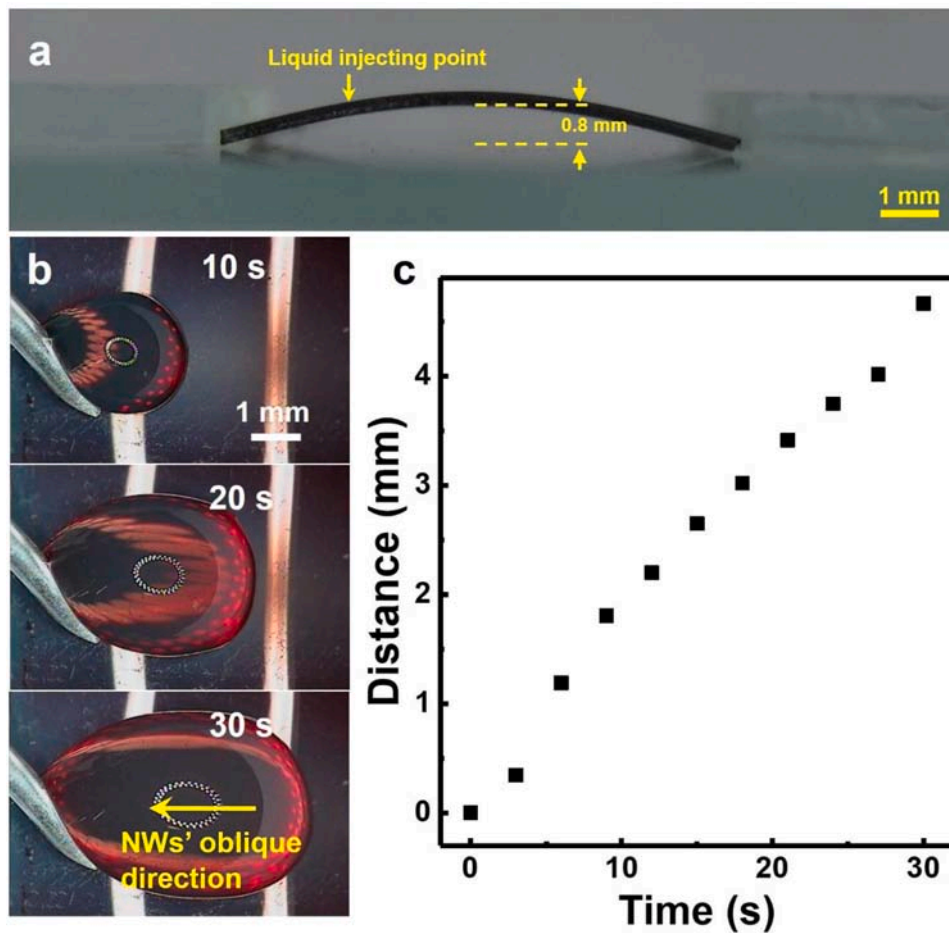


Fig. 4. Water transport on the oblique PI NWs array. (a) Optical image of the bent PI film with oblique NWs array. (b) Optical images of the water droplet added on the film with 1 $\mu\text{L/s}$ speed after 10 s, 20 s and 30 s. (c) Statistic result of the transport distance changing with water adding time.

Combining with the revised equation, we can give a brief quantitative description about the peculiar experimental phenomena.

According to our model, the hysteresis generated by oblique PI NWs array hinders the spread of the droplet to a certain extent, and capillary force plays an important role along the direction parallel to oblique PI NWs arrays. As a result, along the direction perpendicular to NW arrays, the velocity of the droplet on oblique PI NWs array should be much lower than that on bare substrate. This is in accordance with the experimental result where the movement of these two edges of the droplet is invisible. And along the NWs' oblique direction, capillary force is negative, which further hinders the spreading of water droplet. While along NWs' oblique direction, capillary force is positive and promotes spreading of the droplet. Therefore, the droplet shows a preferred unidirectional spreading direction.

When the PI film is tilted, the effect of gravity should also be taken into account. Against NWs' oblique direction, the gravity term is negative, so there is a competition between capillary force and gravity. Their resultant force determines the spreading behavior of water droplet. With the gradual increase of the tilt angle, this resultant force decreases accordingly, which leads to a gradual slowing down of the spreading velocity of the water droplet's top edge. While along NWs' oblique direction, the gravity term is positive, so the resultant force of the capillary term and gravity term increases gradually with the increasing of tilt angle. When the tilt angle is larger than a certain value, droplet starts spreading along this direction.

To quantitatively study the spreading behavior of water droplet on oblique PI NWs array, a simulation is conducted based on the above proposed model. As shown in Fig. 3b, the calculated curve of the average

spreading speed of droplet's top edge with tilt angle fits well with the experiment results, which further proves that the model is reasonable. By now, all experiments and theoretical analysis prove that the capillary force drives water droplet to spread unidirectionally against NWs' oblique direction and even conquers the gravity to make droplet climb up along upright PI film.

3.3. Directional water transportation on oblique PI NWs array

Then, we try to transport water directionally with the oblique PI NWs array. As shown in Fig. 4a, a piece of film is bent into an arc-shape with curvature radius of 2.7 cm, and deionized water was added onto the left side of the film continuously by a needle with the injecting speed of 1 $\mu\text{L/s}$. Fig. 4b and Movie S3 show the water droplet moving from left side to the right side in about 40 s, and Fig. 4c shows the relationship between the moving direction and the time after adding water, the moving speed of the droplet was almost constant with little reduction when passing the arch. This result shows that using the oblique PI NWs array, we can transport water directionally against the NWs' oblique direction.

Anisotropic movement of water on hydrophobically treated oblique PI NWs array

When the oblique PI NWs array was treated hydrophobic, water droplet could no longer spread on its surface, but other interesting anisotropic wetting property emerged. Using a very simple method (shown in the methods), we treated the oblique PI NWs film hydrophobic. As Fig. 5a and 5b show, after the treatment, the morphology of

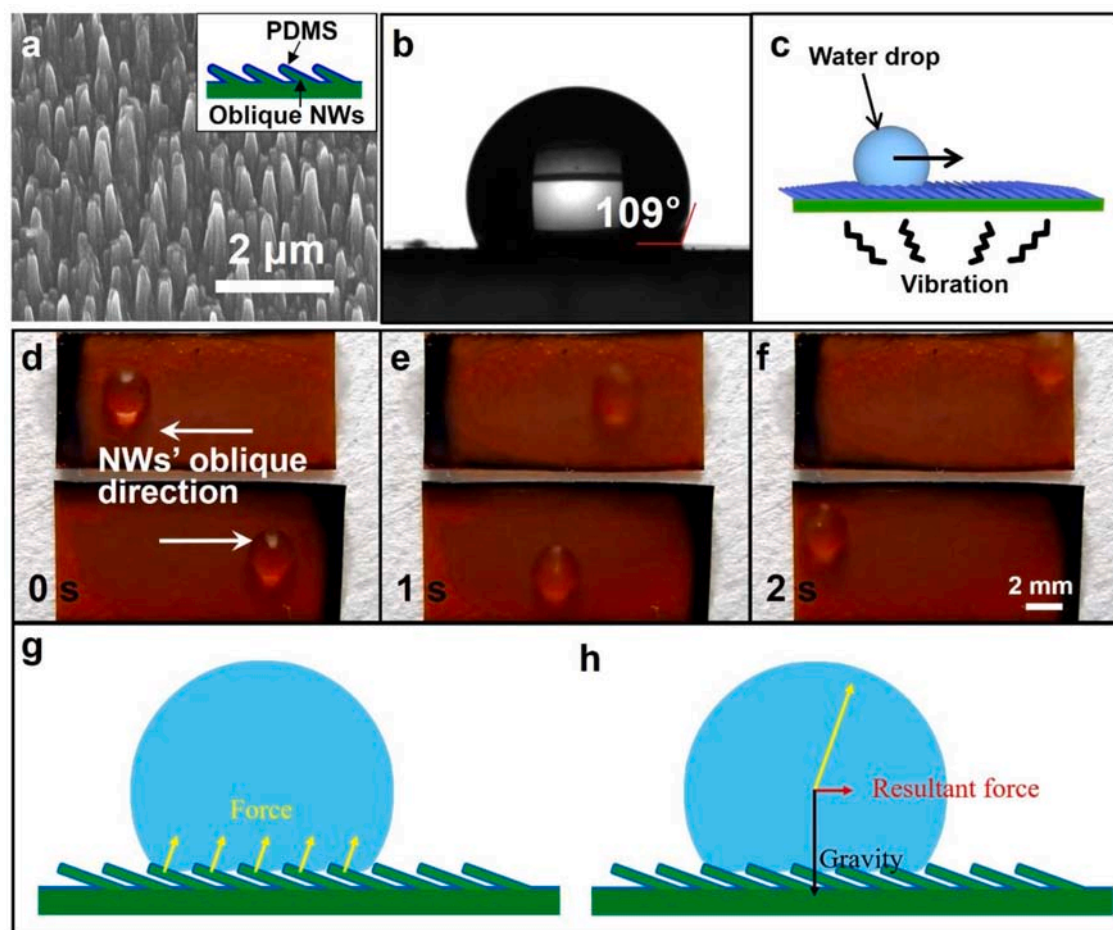


Fig. 5. Movement of water droplet on hydrophobically treated oblique PI NWs array under vibration. (a) Top view SEM image of the hydrophobically treated oblique PI NWs array, the insert shows the structure after treatment. (b) Optical image of 5 μL water droplet on the film, the contact angle is 109° . (c) Schematic diagram of the equipment to test water droplet on the hydrophobically treated oblique PI NWs array moving under vibration (d) to (f) show the optical images of the films with water droplets after 0 s, 1 s and 2 s vibration by sound wave. (g) Contact state of the NWs and the water droplet, and the force applied on the water droplet. (h) Resultant force applied on water droplet.

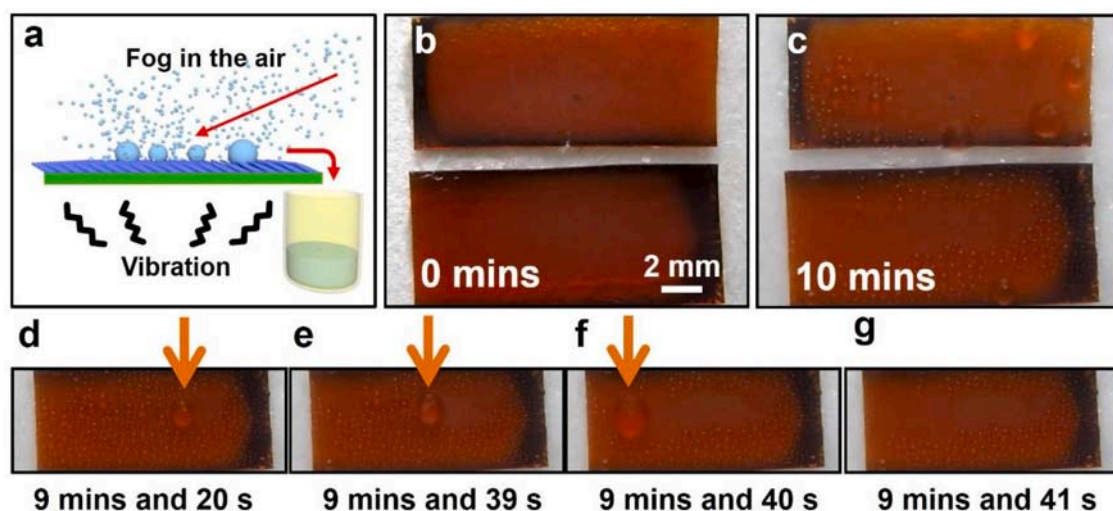


Fig. 6. Fog collection using hydrophobically treated oblique PI NWs array. (a) Schematic diagram of the equipment to collect fog with hydrophobically treated oblique PI NWs array. (b) and (c) show the optical images of the films after 0 min and 10 min, respectively. (d) to (g) show the movement of a water droplet on the film.

the NWs array exhibits no obvious change, but the contact angle of the array to water changes to 109° . In this condition, a water droplet will not spread anisotropically on the film, but will move against the NWs' oblique direction under vibration (schematic diagram of the equipment shown in Fig. 5c) with about the average moving speed of 4 mm/s (shown in Fig. 5d–5f and Movie S4). The directional movement of water droplets on hydrophobically treated oblique PI NWs array could be explained by the following reason (shown in Fig. 5g and 5h): as the NWs array was treated hydrophobic, water contact only with the top side of the NWs (as that shown in Fig. 5g), and thus when the film with oblique PI NWs array vibrates, NWs applied a force perpendicular to the NWs (shown with the yellow arrows in Fig. 5g). Since the gravity balanced the component force perpendicular to the ground, the resultant force applied on the water droplet was horizontal against the oblique direction of NWs (shown in Fig. 5h). Consequently, the water droplet moves directionally against NWs' obliquity under vibration.

Directional fog collection on hydrophobically treated oblique PI NWs array

As small water droplets could move fast on the surface of hydrophobically treated oblique PI NWs array, fog drops coagulating on the film could be accumulated together based on this phenomenon and transported directionally to a collector, which may be useful in fog collection. Based on the theory shown in Fig. 6a, we tried to collect fog with the hydrophobically treated oblique PI NWs array, and transport the collected water directionally under vibration. Fig. 6b–6g and Movie S5 show the process of fog coagulating on the film and the movement of the droplets on the film under vibration. As we can see, with the coagulating of fog drops, water droplets grew on the film and merged with neighboring droplets. When the water droplets grow large enough, they start moving, joining the other droplets in their path, and finally taking the collected water out of the film against the NWs' oblique direction. In this case, the droplets could be collected easily by a collector.

4. Conclusion

In summary, we fabricated oblique PI NWs array and studied its anisotropic wetting properties. Water droplets dropped on the oblique PI NWs array spread anisotropically on the surface, with their edge spreading against the NWs' oblique direction. Water droplets could spread up even when the film was set perpendicular to the ground. Theoretical research shows that unidirectional spreading of water droplets was mainly caused by the capillary force generated by the oblique PI NWs array. The oblique PI NWs array could be easily treated hydrophobic on which water droplets moving directionally against NWs' obliquity under vibration. Furthermore, we exhibited the potential to apply the oblique PI NWs array on water transport and fog collection. As the NWs array could be easily fabricated on PI films, this material might be very useful in these large-scale applications which need simple manufacturing process and high production.

Declaration of Competing Interest

The authors declare that they have no known competing financial interests or personal relationships that could have appeared to influence the work reported in this paper.

Acknowledgements

We thank Yingdong Li of Beijing Ion Beam Technology Co., Ltd. for his help in the experiment.

Funding

This work was supported by the National Natural Science Foundation of China (grant number 51702377), Joint fund of Equipment pre-

Research and Ministry of Education (grant number 6141A02022518), the National Program for Support of Top-notch Young Professionals, and the Fundamental Research Funds for the Central Universities (grant number lzujbky-2018-ot04).

Supplementary materials

Supplementary material associated with this article can be found, in the online version, at doi:10.1016/j.surfin.2020.100784.

References

- [1] X.-M. Li, D. Reinhoudt, M. Crego-Calama, What do we need for a superhydrophobic surface? A review on the recent progress in the preparation of superhydrophobic surfaces, *Chem. Soc. Rev.* 36 (2007) 1350–1368, <https://doi.org/10.1039/B602486F>.
- [2] S. Das, S. Kumar, S.K. Samal, S. Mohanty, S.K. Nayak, A Review on Superhydrophobic Polymer Nanocoatings: Recent Development and Applications, *Ind. Eng. Chem. Res.* 57 (2018) 2727–2745, <https://doi.org/10.1021/acs.iecr.7b04887>.
- [3] A. Lafuma, D. Quere, Superhydrophobic states, *Nat. Mater.* 2 (2003) 457–460, <https://doi.org/10.1038/nmat924>.
- [4] K. Koch, W. Barthlott, Superhydrophobic and superhydrophilic plant surfaces: an inspiration for biomimetic materials, *Philos. Trans. R. Soc. A-Math. Phys. Eng. Sci.* 367 (2009) 1487–1509, <https://doi.org/10.1098/rsta.2009.0022>.
- [5] J. Rafiee, M.A. Rafiee, Z.-Z. Yu, N. Koratkar, Superhydrophobic to Superhydrophilic Wetting Control in Graphene Films, *Adv. Mater.* 22 (2010) 2151–2154, <https://doi.org/10.1002/adma.200903696>.
- [6] M. Gleiche, L.F. Chi, H. Fuchs, Nanoscopic channel lattices with controlled anisotropic wetting, *Nature* 403 (2000) 173–175, <https://doi.org/10.1038/35003149>.
- [7] L. Courbin, E. Denieul, E. Dressaire, M. Roper, A. Ajdari, H.A. Stone, Imbibition by polygonal spreading on microdecorated surfaces, *Nat. Mater.* 6 (2007) 661–664, <https://doi.org/10.1038/nmat1978>, 661–664.
- [8] N.A. Malvadkar, M.J. Hancock, W.J. Dressick, M.C. Demirel, An engineered anisotropic nanofilm with unidirectional wetting properties, *Nat. Mater.* 9 (2010) 1023–1028, <https://doi.org/10.1038/nmat2864>.
- [9] M. Tenjimabayashi, M. Higashi, T. Yamazaki, I. Takenaka, T. Matsubayashi, T. Moriya, M. Komine, R. Yoshikawa, K. Manabe, S. Shiratori, Droplet Motion Control on Dynamically Hydrophobic Patterned Surfaces as Multifunctional Liquid Manipulators, *ACS Appl. Mater. Interfaces* 9 (2017) 10371–10377, <https://doi.org/10.1021/acsami.7b01641>.
- [10] Y. Cui, D.W. Li, H. Bai, Bioinspired Smart Materials for Directional Liquid Transport, *Ind. Eng. Chem. Res.* 56 (2017) 4887–4897, <https://doi.org/10.1021/acs.iecr.7b00583>.
- [11] Y. Zheng, H. Bai, Z. Huang, X. Tian, F.-Q. Nie, Y. Zhao, J. Zhai, L. Jiang, Directional water collection on wetted spider silk, *Nature* 463 (2010) 640–643, <https://doi.org/10.1038/nature08729>.
- [12] J. Ju, H. Bai, Y. Zheng, T. Zhao, R. Fang, L. Jiang, A multi-structural and multi-functional integrated fog collection system in cactus, *Nat. Commun.* 3 (2012) 1247, <https://doi.org/10.1038/ncomms2253>.
- [13] P. Zhang, L. Zhang, H. Chen, Z. Dong, D. Zhang, Surfaces Inspired by the Nepenthes Peristome for Unidirectional Liquid Transport, *Adv. Mater.* 29 (2017), 1702995, <https://doi.org/10.1002/adma.201702995>.
- [14] Y. Yang, X. Li, X. Zheng, Z. Chen, Q. Zhou, Y. Chen, 3D-Printed Biomimetic Super-Hydrophobic Structure for Microdroplet Manipulation and Oil/Water Separation, *Adv. Mater.* 30 (2018), 1704912, <https://doi.org/10.1002/adma.201704912>.
- [15] G. Sun, Y. Fang, Q. Cong, L.-q. Ren, Anisotropism of the Non-Smooth Surface of Butterfly Wing, *J. Bionic Eng.* 6 (2009) 71–76, [https://doi.org/10.1016/S1672-6529\(08\)60094-3](https://doi.org/10.1016/S1672-6529(08)60094-3).
- [16] Y. Zheng, X. Gao, L. Jiang, Directional adhesion of superhydrophobic butterfly wings, *Soft Matter* 3 (2007) 178–182, <https://doi.org/10.1039/B612667G>.
- [17] S.Y. Deng, W.F. Shang, S.L. Feng, S.P. Zhu, Y. Xing, D. Li, Y.P. Hou, Y.M. Zheng, Controlled droplet transport to target on a high adhesion surface with multi-gradients, *Sci. Rep.* 7 (2017) 45687, <https://doi.org/10.1038/srep45687>.
- [18] J.B. Wu, L.B. Zhang, Y.C. Wang, P. Wang, Efficient and Anisotropic Fog Harvesting on a Hybrid and Directional Surface, *Adv. Mater. Interfaces* 4 (2017), 1600801, <https://doi.org/10.1002/admi.201600801>.
- [19] K.-C. Park, P. Kim, A. Grinthal, N. He, D. Fox, J.C. Weaver, J. Aizenberg, Condensation on slippery asymmetric bumps, *Nature* 531 (2016) 78–82, <https://doi.org/10.1038/nature16956>.
- [20] K.-H. Chu, R. Xiao, E.N. Wang, Uni-directional liquid spreading on asymmetric nanostructured surfaces, *Nat. Mater.* 9 (2010) 413–417, <https://doi.org/10.1038/nmat2726>.
- [21] T.-i. Kim, K.Y. Suh, Unidirectional wetting and spreading on stooped polymer nanohairs, *Soft Matter* 5 (2009) 4131–4135, <https://doi.org/10.1039/B915079J>.
- [22] H. Geng, Y. Fan, S. Wang, T. Ba, C. Yu, M. Cao, L. Jiang, Unidirectional water delivery on a superhydrophilic surface with two-dimensional asymmetrical wettability barriers, *Mater. Horiz.* 5 (2018) 303–308, <https://doi.org/10.1039/C7MH01138E>.

- [23] Y. Si, T. Wang, C. Li, C. Yu, N. Li, C. Gao, Z. Dong, L. Jiang, Liquids Unidirectional Transport on Dual-Scale Arrays, *ACS Nano* 12 (2018) 9214–9222, <https://doi.org/10.1021/acsnano.8b03924>.
- [24] Z. Zhao, C. Li, Z. Dong, Y. Yang, L. Zhang, S. Zhuo, X. Zhou, Y. Xu, L. Jiang, M. Liu, Adaptive Superamphiphilic Organohydrogels with Reconfigurable Surface Topography for Programming Unidirectional Liquid Transport, *Adv. Funct. Mater.* 29 (2019), 1807858.
- [25] X. Zhang, D. Wang, Y. Zhang, D. Zhang, Z. Li, H. Liu, Bioinspired Unidirectional Liquid Spreading Channel-Principle, Design, and Manufacture, *Adv. Mater. Interfaces* 7 (2020), 1901791, <https://doi.org/10.1002/admi.201901791>.
- [26] H. Chen, L. Zhang, P. Zhang, D. Zhang, Z. Han, L. Jiang, A Novel Bioinspired Continuous Unidirectional Liquid Spreading Surface Structure from the Peristome Surface of *Nepenthes alata*, *Small* 13 (2017), 1601676, <https://doi.org/10.1002/sml.201601676>.
- [27] T.Q. Wang, H.X. Chen, K. Liu, S.L. Wang, P.H. Xue, Y. Yu, P. Ge, J.H. Zhang, B. Yang, Janus Si Micropillar Arrays with Thermal-Responsive Anisotropic Wettability for Manipulation of Microfluid Motions, *ACS Appl. Mater. Interfaces* 7 (2015) 376–382, <https://doi.org/10.1021/am5063647>.
- [28] S. Huang, J.L. Song, Y. Lu, C.J. Lv, H.X. Zheng, X. Liu, Z.J. Jin, D.Y. Zhao, C. J. Carmalt, I.P. Parkin, Power-free water pump based on a superhydrophobic surface: generation of a mushroom-like jet and anti-gravity long-distance transport, *J. Mater. Chem. A* 4 (2016) 13771–13777, <https://doi.org/10.1039/C6TA04908G>. DOI.
- [29] W. Wu, L. Cheng, S. Bai, Z.L. Wang, Y. Qin, Directional Transport of Polymer Sheet and a Microsphere by a Rationally Aligned Nanowire Array, *Adv. Mater.* 24 (2012) 817–821, <https://doi.org/10.1002/adma.201104085>.
- [30] L. Cheng, W. Dou, S. Bai, W. Wu, Q. Xu, Y. Qin, Controllable Fabrication of Patterned Oblique Nanowire Array and Its Application as a Reflection Grating, *Sci. Adv. Mater.* 5 (2013) 1179–1183, <https://doi.org/10.1166/sam.2013.1570>.
- [31] P.G. Degennes, Wetting - Statics and Dynamics, *Rev. Mod. Phys.* 57 (1985) 827–863, <https://doi.org/10.1103/RevModPhys.57.827>.